

# Metal-Grating-Coupled Terahertz Quantum-Well Photodetectors

R. Zhang, X. G. Guo, C. Y. Song, M. Buchanan, Z. R. Wasilewski, J. C. Cao, and H. C. Liu, *Fellow, IEEE*

**Abstract**—Three terahertz (THz) GaAs/AlGaAs quantum-well photodetectors with different 1-D metal gratings are fabricated for front-incident detection of THz waves. Photocurrent spectra are acquired and compared with 45° incident facet samples (without grating), and peak responsivities are determined with a calibrated blackbody radiation source. The results show that these gratings can couple THz waves into detectors effectively, resulting in good detector responsivities. The modal method is employed to simulate the light coupling efficiency and the optimization conditions of the gratings.

**Index Terms**—Detector, grating, quantum well (QW), terahertz (THz).

## I. INTRODUCTION

TERAHERTZ (THz) quantum-well photodetectors (QWPs) [1]–[3] have been recently demonstrated, which are of importance for constructing fast, compact, and integrated THz application systems. The intersubband-transition selection rule makes THzQWPs insensitive to the radiation incident from the direction normal to the quantum-well (QW) plane [4], [5], whereas in focal-plane array (FPA) applications, the THz wave is close to normal incidence onto the device. Thus, a light coupler, such as grating, is necessary to obtain the radiation propagating parallel to the QW layers.

Manuscript received January 17, 2011; accepted January 29, 2011. Date of publication March 21, 2011; date of current version April 27, 2011. This work was supported in part by the National Basic Research Program of China under Grant 2007CB310402, by the 863 Program of China, by the National Natural Science Foundation of China under Grant 60721004, by the major projects (Project Nos. KGCX1-YW-24 and KGCX2-YW-231) and the Hundred Talent Program of the Chinese Academy of Sciences, and by the Shanghai Municipal Commission of Science and Technology Project 10JC1417000. The review of this paper was arranged by Editor C. Jagadish.

R. Zhang and X. G. Guo are with the Key Laboratory of Terahertz Solid-State Technology, Shanghai Institute of Microsystem and Information Technology, Chinese Academy of Sciences, Shanghai 200050, China and also with the Institute for Microstructural Sciences, National Research Council, Ottawa, ON K1A 0R6, Canada.

C. Y. Song, M. Buchanan, and Z. R. Wasilewski are with Institute for Microstructural Sciences, National Research Council, Ottawa, ON K1A 0R6, Canada.

J. C. Cao is with the Key Laboratory of Terahertz Solid-State Technology, Shanghai Institute of Microsystem and Information Technology, Chinese Academy of Sciences, Shanghai 200050, China.

H. C. Liu is with the Institute for Microstructural Sciences, National Research Council, Ottawa, ON K1A 0R6, Canada and also with the Key Laboratory of Artificial Structures and Quantum Control (Ministry of Education), Department of Physics, Shanghai Jiao Tong University, Shanghai 200240, China (e-mail: H.C.Liu@sjtu.edu.cn)

Color versions of one or more of the figures in this letter are available online at <http://ieeexplore.ieee.org>.

Digital Object Identifier 10.1109/LED.2011.2112632

TABLE I  
PARAMETERS OF THE THREE THzQWP WAFERS

Wafer	$L_w$ (Å)	$L_b$ (Å)	Repeat N	[Al]	$N_d$ (cm <sup>-3</sup> )
V266	155	702	30	3%	$6 \times 10^{16}$
V267	221	951	23	1.5%	$3 \times 10^{16}$
V458	195	830	32	2%	$1.5 \times 10^{17}$

$L_w$  is the GaAs quantum well width,  $L_b$  is the AlGaAs barrier width, repeat N is the period number of  $L_w+L_b$ , [Al] is the barrier Al fraction,  $N_d$  is the doping density in the center 100 Å of the quantum well.

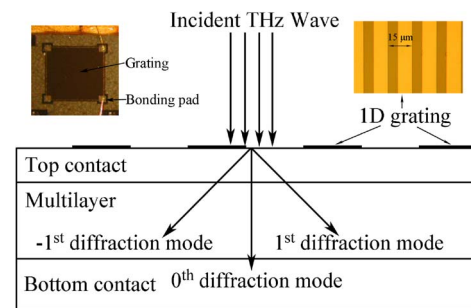


Fig. 1. Schematic of the metal-grating-coupled THzQWP. (Insets) Left: top view of the mesa; right: microscope picture of the grating.

Recently, Patrashin and Hosako [6] have reported a 1-D grating THzQWP with a 13-mA/W peak responsivity at a bias of 40 mV and an operating temperature of 3 K. In this letter, three different 1-D grating THzQWPs are fabricated and studied. Much higher peak responsivities than that in [6] are obtained. The modal method [7] is employed to analyze the results, and the design and the optimization are also discussed. Our findings provide a promising way to realize highly efficient frontside-illuminated THzQWPs.

## II. DEVICE DESIGN

Three wafers (V266, V267, and V458) were grown by molecular beam epitaxy on semi-insulating GaAs substrates, and mesa devices were fabricated by standard GaAs processing techniques. The mesas are  $1500 \mu\text{m} \times 1500 \mu\text{m}$  squares, and the grating metal is Ti/Pt/Au [25/55/300 nm], defined on the top of the mesa. The QWs are sandwiched between 4000 and 8000 Å of the top and bottom contacts, doped to  $10^{17} \text{cm}^{-3}$ . Other design parameters are given in Table I. A schematic of the grating THzQWP is shown in Fig. 1.

The gratings are designed according to the following diffraction equation:

$$m\lambda = nd(\sin \alpha + \sin \beta) \quad (1)$$

TABLE II  
GRATING PARAMETERS. THE REFRACTIVE  
INDEX OF GAAS IS TAKEN AS 3.2

Sample ID	Response Peak (THz)	Design (THz)	Grating Period ( $\mu\text{m}$ )
V266-G20	5.4	3.8	20
V267-G33	3.2	1.9	33
V458-G20	$\sim 5.5$	3.8	20

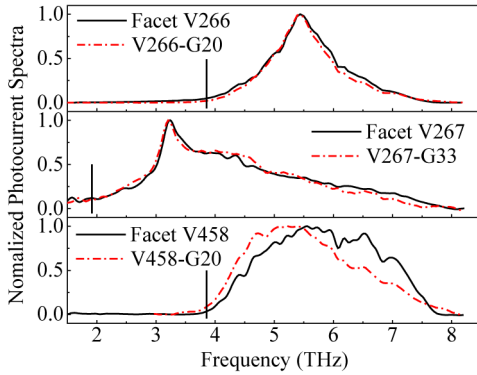


Fig. 2. Normalized photocurrent spectra of (black line) facet THzQWPs and (red dash-dotted line) grating THzQWPs at 8 K. The spectra of facet samples are taken under the  $45^\circ$ -incident configuration. (Vertical lines) Frequencies used for grating designs. The spectra of grating samples are taken under the normal incidence.

where  $m$  is the diffraction order,  $\lambda$  is the wavelength of incident wave,  $n$  is the refractive index,  $d$  is the period of the 1-D grating, and  $\alpha$  and  $\beta$  are the incident and diffractive angles, respectively. For the normal incidence and taking the first diffraction order, we set  $m = 1$ ,  $\alpha = 0$ , and  $\beta = 90^\circ$  to get the period of the grating, i.e.,

$$d \approx \frac{\lambda_{\max}}{n}. \quad (2)$$

$\lambda_{\max}$  is usually called the cutoff of the grating, i.e., all wavelengths shorter than  $\lambda_{\max}$  are diffracted. The design parameters of gratings are given in Table II.

### III. RESULTS AND DISCUSSIONS

The response peaks in Table II are acquired from the photocurrent spectra of the corresponding facet samples ( $45^\circ$  incidence), which are shown in Fig. 2 (black line). The designed frequencies are lower than the peak response frequencies. According to (2), the designed frequency corresponding to  $\lambda_{\max}$  should make the grating effective over the entire response region. This can be easily understood from the vertical lines in Fig. 2. The filling factors of the gratings are set to be around 50%. The measured spectra of grating samples are also given in Fig. 2 (red dash-dotted line). It is shown that the two series of spectra are nearly the same, which indicates that our gratings can couple the THz waves into THzQWPs effectively. It should be noted that the broader response of V458 is due to the relative higher doping density [8]. Heavier doping gives stronger scattering and, therefore, broader response.

Based on the spectra of grating samples in Fig. 2, the peak responsivities were determined with a calibrated blackbody radiation source (shown in Fig. 3). These values may be im-

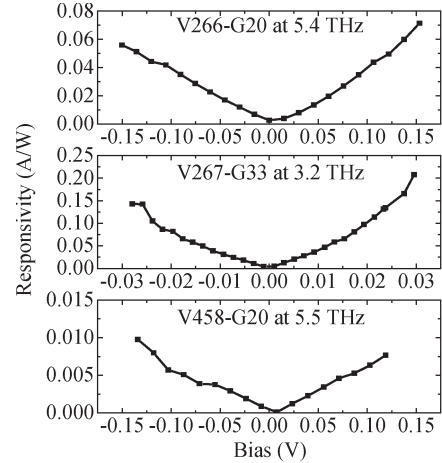


Fig. 3. Peak responsivities of three grating THzQWPs versus bias. All measurements are taken at 4.3 K.

proved because the gratings here are designed according to the simple diffraction equation. In order to optimize the coupling efficiency of the gratings, the modal method [7] is employed to study the electromagnetic field in the samples.

We simulate the coupling efficiency of the gratings. The dielectric function of GaAs is taken from [9], and the one of the metal is provided by the Drude model. At the metal/semiconductor interface, the surface impedance boundary condition [7] is used to take into account the dissipation of the metal, which can also include the near-field effects such as the enhancement by the presence of surface plasmons. We find that, when the period of the grating is equal to the wavelength of the THz wave in the sample material (GaAs here), the coupling efficiency reaches a maximum. Therefore, for a grating with a period of  $d$ , where  $\lambda_{\max}$  from (2) is not the cutoff, it is found that, on the contrary, THz waves with  $\lambda_{\max}$  are coupled by the grating most efficiently. However, for the case of V266-G20, where the period of the grating is  $20 \mu\text{m}$  corresponding to the wavelength of 3.8 THz in GaAs, this does not match the response peak of V266 at 5.4 THz. The gratings simply designed by the diffraction equation are not the most efficient ones, and this affects the detector's responsivity. According to the numerical result, the period of the grating should be set to match the peak response frequency. For V266, it is around  $14.6 \mu\text{m}$ . Moreover, because of the long wavelength and the near-field effect, simulations show that these gratings are also effective for wavelengths longer than  $\lambda_{\max}$ . To confirm these predictions, we fabricated two additional samples (V266-G12 with a  $12\text{-}\mu\text{m}$ -period grating and V266-G15 with a  $15\text{-}\mu\text{m}$ -period grating). The ratio of simulated coupling efficiencies at 5.4 THz is 1.58 : 3.27 : 1 for V266-G12, V266-G15, and V266-G20. The measured photocurrent spectra are given in Fig. 4(a).

It is shown that the photocurrent spectrum of V266-G12 is distorted, whereas for V266-G15, the shape remains nearly the same and only shows a small red shift. The vertical lines indicating the positions of gratings are shown to help explain the distortion. According to our numerical simulation, the incident waves with the frequency indicated by the vertical lines are most efficiently coupled by the following gratings: 5.28 THz for the  $15\text{-}\mu\text{m}$ -period grating (red dash-dotted line) and 6.27 THz

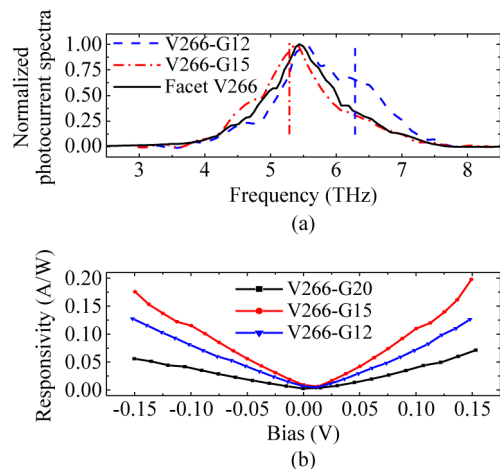


Fig. 4. (a) Normalized photocurrent spectra of (blue dashed line) V266-G12 and (red dash-dotted line) V266-G15. (Black line) The one of facet sample is also given for comparison. (Vertical lines) Cutoff of two gratings: (blue) 12- $\mu\text{m}$ -period grating; (red) 15- $\mu\text{m}$ -period grating. (b) Peak responsivities of V266-G12 and V266-G15. The one of V266-G20 is from Fig. 3 for comparison.

for the 12- $\mu\text{m}$ -period grating (blue dashed line), respectively. Due to this, a shoulder appears around the blue vertical line in the spectrum of V266-G12, whereas for V266-G15, because the red vertical line is close to the peak response frequency of V266, no significant distortion is observed. This effect also influences the spectrum of V458-G20 (as in Fig. 2). The response shape is skewed toward the grating position (3.8 THz). For the cases of V266-G20 and V267-G33, the spectra are similar to the facet ones. The possible reason is that the spectra for these two are sharply peaked and, hence, the effect of the grating is not clearly visible. Another feature in Fig. 4(a) is that  $\lambda_{\text{max}}$  from (2) is confirmed not to be the cutoff and THz waves with a longer wavelength can be also coupled by the gratings due to the near-field effects. Based on the spectra in Fig. 4(a), peak responsivities of V266 with different gratings are acquired [see Fig. 4(b)]. At a 0.15-V bias, the results are 0.128, 0.197, and 0.070 A/W for V266-G12, V266-G15, and V266-G20, respectively, and the ratio is 1.83:2.81:1. It is shown that general behaviors of the experiments and the simulations agree, and the 15- $\mu\text{m}$ -period grating is the most efficient one. The estimated detectivity is more than  $10^{11}$  cm Hz<sup>1/2</sup>/W at 4.2 K. Compared with commercialized bolometers, which are intrinsically slow due to their heat-based detection schemes, and Schottky-barrier-diode THz detectors [10], [11], the performance of which greatly decreases with increasing frequency, grating THzQWPs are high-response and high-speed detectors. It is worth noting that the value of 0.197 A/W is not as good as that of the 45° facet sample, which is 0.428 A/W by measure-

ment. However, in FPA-based applications such as real-time imaging, the normal incidence is required, and a light coupler such as grating is necessary. Moreover, thinning the substrate would further improve the performance to that comparable with the facet. It is our past experience that optimized gratings gave comparable responsivity as the facet.

#### IV. CONCLUSION

In conclusion, we have studied THzQWPs with 1-D metal gratings and have demonstrated that 1-D gratings can couple the light into the devices effectively. Optimizations of the gratings have been discussed based on numerical simulations and experimental results. We have found that the THz wave with the frequency at the cutoff of the grating is actually most efficiently diffracted; to improve the detector's responsivity, the period of the grating should match the response peak of the detector. As an example of our results, for V266, the coupling efficiency is almost three times higher for a 15- $\mu\text{m}$ -period grating than for a 20- $\mu\text{m}$ -period grating (with a peak responsivity reaching 0.197 A/W at 0.15 V).

#### REFERENCES

- [1] H. C. Liu, C. Y. Song, A. J. SpringThorpe, and J. C. Cao, "Terahertz quantum-well photodetector," *Appl. Phys. Lett.*, vol. 84, no. 20, pp. 4068–4070, May 2004.
- [2] H. Luo, H. C. Liu, C. Y. Song, and Z. R. Wasilewski, "Background-limited terahertz quantum-well photodetector," *Appl. Phys. Lett.*, vol. 86, no. 23, pp. 231 103-1–231 103-3, Jun. 2005.
- [3] M. Graf, G. Scalari, D. Hofstetter, J. Faist, H. Beere, E. Linfield, D. Ritchie, and G. Davies, "Terahertz range quantum well infrared photodetector," *Appl. Phys. Lett.*, vol. 84, no. 4, pp. 475–477, Jan. 2004.
- [4] H. C. Liu, M. Buchanan, and Z. R. Wasilewski, "How good is the polarization selection rule for intersubband transitions?" *Appl. Phys. Lett.*, vol. 72, no. 14, pp. 1682–1684, Apr. 1998.
- [5] H. Schneider and H. C. Liu, *Quantum Well Infrared Photodetectors: Physics and Applications*. Berlin, Germany: Springer-Verlag, 2006, pp. 13–17.
- [6] M. Patrashin and I. Hosako, "Terahertz frontside-illuminated quantum-well photodetector," *Opt. Lett.*, vol. 33, no. 2, pp. 168–170, Jan. 2008.
- [7] Y. Todorov and C. Minot, "Modal method for conical diffraction on a rectangular slit metallic grating in a multilayer structure," *J. Opt. Soc. Amer. A, Opt. Image Sci.*, vol. 24, no. 10, pp. 3100–3114, Oct. 2007.
- [8] H. C. Liu, R. Dudek, A. Shen, E. Dupont, C. Y. Song, Z. R. Wasilewski, and M. Buchanan, "High absorption (>90%) quantum-well infrared photodetectors," *Appl. Phys. Lett.*, vol. 79, no. 25, pp. 4237–4239, Dec. 2001.
- [9] J. S. Blakemore, "Semiconducting and other major properties of gallium arsenide," *J. Appl. Phys.*, vol. 53, no. 10, pp. R123–R181, Oct. 1982.
- [10] L. Liu, J. L. Hesler, H. Xu, A. W. Lichtenberger, and R. M. Weikle, II, "A broadband quasi-optical terahertz detector utilizing a zero bias Schottky diode," *IEEE Microw. Wireless Compon. Lett.*, vol. 20, no. 9, pp. 504–506, Sep. 2010.
- [11] F. Sizov and A. Rogalski, "Terahertz detectors," *Prog. Quantum Electron.*, vol. 34, no. 5, pp. 278–347, Sep. 2010.